AAS 11-225

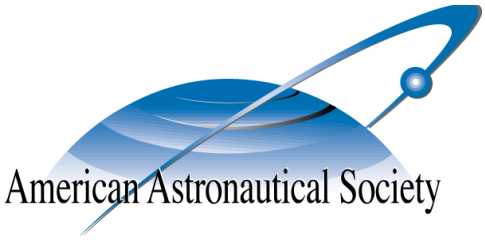

American Institute of
Aeronautics and Astronautics

LINEAR STABILITY AND SHAPE ANALYSIS OF SPINNING THREE-CRAFT COULOMB FORMATIONS

Erik Hogan and Hanspeter Schaub

University of Colorado, Boulder, CO 80309-0431

AAS/AIAA Astrodynamics Specialists Conference

New Orleans, Louisiana August 18–21, 2008

AAS Publications Office, P.O. Box 28130, San Diego, CA 92198

AAS 11-225

LINEAR STABILITY AND SHAPE ANALYSIS OF SPINNING THREE-CRAFT COULOMB FORMATIONS

Erik Hogan* **and Hanspeter Schaub†**
University of Colorado, Boulder, CO 80309-0431

This paper describes the discovery of families of multiple invariant shape solutions for collinear three-craft Coulomb formations with set charges, as well as the results of linear stability analysis on such formations. The charged spacecraft are assumed to be spinning about each other in deep space without relevant gravitational forces present. Up to three invariant shape solutions are possible for a single set of craft charges. This behavior, only speculated in previous work, is confirmed through analysis and numerical simulation examples. In fact, distinct regions are analytically described where two or three invariant shape solutions exist for a single charge set. These regions are analyzed to determine what range of trajectories are possible. Linear stability analysis yields the first examples of marginally stable three-craft invariant shape formations. Linearly stable behavior is only observed when two invariant shape solutions result for one set of charges, where one shape will be unstable and the other marginally stable. Numerical simulation illustrates stability for ten orbital periods.

INTRODUCTION

Close formation flying of spacecraft within dozens of meters presents many exciting possibilities, with applications ranging from advanced weather monitoring to high resolution Earth imaging and astronomy applications. The ability to concentrate a large number of scientific instruments within a group of satellites separated by tens of meters would be a major step forward over the limited space provided by a single satellite. A further advantage of using a satellite formation results from the fact that not all of the satellites need to be launched simultaneously. This means that an advanced complex of scientific instrumentation could be pieced together gradually over time. Because the satellite formation would not need to be connected by a rigid structure, a large savings in mass can occur over a large single body structure. With the high cost of sending objects into orbit, any reduction in mass results in a significant reduction in cost. This makes space-based science missions more economical, allowing for a larger number of studies to be conducted. One potential application where close formation flights would be particularly useful is the field of interferometry. In fact, such formations have been proposed for the Terrestrial Planet Finder Interferometer concept currently under study by NASA.[1,2]

Many instruments used to conduct space based research can be very sensitive to interference caused by free floating particles. When considering close formation flight of a small cluster of satellites, this can be a very serious problem if traditional propellant-type thrusters are used to

*Graduate Student, Department of Aerospace Engineering Sciences, University of Colorado
†Associate Professor, H. Joseph Smead Fellow, Department of Aerospace Engineering Sciences, University of Colorado, 431 UCB, Colorado Center for Astrodynamics Research, Boulder, CO 80309-0431

maintain the formation. In such close proximity, it is feasible that the propellant mass ejected by a thruster on one satellite will come into contact with other satellites and possibly interfere with the delicate instrumentation onboard. One way to circumvent this problem is to use electrostatic forces to control the formation.[3,4] By charging individual spacecraft, attractive and repulsive forces are created which can be used to control a close formation at distances up to tens of meters.[5] This method of propulsion requires essentially no propellant, meaning there will be neglibible ejected particles to interfere with other craft in the formation. Furthermore, it is also very energy efficient, requiring power levels on the order of Watts.[6] Such a propulsion method would require active charge control, which has already been demonstrated on the SCATHA and ATS missions in the 1970s,[7–9] as well as in the ongoing European CLUSTERS mission.[10]

For the current study, we consider three-craft collinear invariant shape Coulomb formations in deep space, where the craft orbit about their collective center of mass. In the original work with such formations, Hussein and Schaub lay the theoretical foundation for determining invariant shape solutions for the three-craft Coulomb formation.[11] Numerical simulation is used to illustrate a few particular invariant shapes, solving for shapes when craft charges are specified. Hogan and Schaub carry the analysis further, considering the problem from a mission design perspective.[12] Here a method is established to solve for craft charges when a particular invariant shape geometry is desired, and prove that for any desired invariant collinear shape a real charge solution always exists. In Reference 11 the authors show that multiple invariant shape solutions might be possible for a single set of craft charges, but no such cases are shown to actually exist. Further, the few collinear solutions numerically simulated were all determined to be unstable.[13] In contrast, the current study seeks to investigate under what conditions families of multiple invariant shape solutions do exist for the spinning collinear charged 3-craft problem. Further, their linear stability properties are of interest to investigate if it is possible to create marginally stable spinning charged spacecraft clusters. The only passively stable charged cluster has been the two-craft configuration discussed in Reference 14. For charge spacecraft clusters with more than 2 components determining passively stable configurations has been elusive.

The charged three-body problem can be considered as an extension of the classical gravitational three-body problem as discussed in References 15, 16, and 17. In Reference 15, the authors consider the gravitational restricted three-body problem modified to include charges on the bodies. In this restricted system, the new libration points are analyzed for stability in the presence of the introduced Coulomb forces. In Reference 16, the authors identify central configurations which exist in the charged three-body problem, where both gravitational and Coulomb forces are present. This work is extended in Reference 17, where stability of these central configurations is studied. Linearly stable and unstable central configurations are found. Each of these works considers not only the electrostatic forces between charged bodies, but also the gravitational forces. It is the treatment of this gravitational attraction that distinguishes the previous research from our current study. Considering both gravitational and Coulomb forces allows more forces to be considered to stabilize the cluster shape. This is observed in Reference 17, where a non-planar relative equilibrium is made possible by this fact. Furthermore, the inclusion of gravity allows for mutual attraction between all three bodies. In our current study, we assume the masses of the bodies are so small (on the order of 100s of kilograms) that the gravitational forces are negligible and only Coulomb forces affect the evolution of the system. With a cluster of more than two spacecraft this means that we are always guaranteed to have repulsion between at least two of the bodies, since two of the craft must always be charged to the same polarity. The current research investigates if linearly stable collinear central

configurations (invariant shape solutions) are feasible which do not require gravitational attraction between the bodies. In the classic gravitational three-body problem only one invariant shape solution results for a given set of body masses.[18] The current study investigates if with electrostatically charged 3-craft clusters it is possible for a set of charges to yield more than one invariant shape solution.

A few important assumptions are invoked in the analysis of the presented work. First, only the case where all three craft are of equal mass is considered. This assumption simplifies the analysis to the point where insightful analytical solutions are feasible. Second, no significant Debye shielding effects are are present. This assumption is justified considering the deep space space weather environment, and the large kilo-Volt range potentials being considered. Lastly, the linearization analysis is performed only for the case where the craft are in a circular invariant shape formation. These assumptions were used in order to provide more analytic insight into the problem, and also to provide a simplified search space when identifying multiple invariant shape solutions for a given set of charges.

The paper is structured as follows. First, the mathematics of invariant shape Coulomb formations are reviewed. Next, the rotating coordinate frame and resulting equations of motion used to analyze the stability of the invariant shapes are presented. Following this, the procedure used to identify multiple invariant shape solutions and present the results of the numerical search is outlined. Lastly, linearization is investigated to analyze a multiple invariant shape solution case, and comment on numerical search results for the stability of different families of multiple invariant shape solutions.

BACKGROUND

Invariant Shape Formation

Let us consider a formation of three charged craft operating in deep space as shown in Fig. 1. The position of each craft with respect to the formation center of mass is defined as $\mathbf{r}_i$. The relative position between craft i and j is denoted as $\mathbf{r}_{ij} = \mathbf{r}_j - \mathbf{r}_i$. Each craft has a mass m_i and a charge q_i. The formation is assumed to be in deep space, thus the gravitational interactions with massive celestial bodies is not considered. Hussein and Schaub[11] lay the groundwork for determining invariant-shape spinning Coulomb formations, where the necessary conditions for such formations to exist are derived in the absence of external perturbations. In the current work this assumption is maintained, as the same conditions are used to formulate the problem under consideration. In the absence of perturbations, the system evolves solely under the influence of electrostatic forces between the craft. In an invariant shape solution all craft maintain constant charge values, denoted as q_i, for all time.

It is important to recognize that invariant shape does not imply a fixed shape. That is, the formation geometry at some time t_i does not necessarily have to match that at some other time, t_j. To clarify the meaning of invariant shape, consider a collinear configuration of craft, as shown in Fig. 2. If we define a parameter, χ, as

$$\chi = \frac{r_{23}}{r_{21}}, \tag{1}$$

then an invariant shape formation is one where χ is constant for all time. The individual separation distances can change with time, so long as the ratio of one to the other remains unchanged. It is apparent that due to separation distances being positive quantities, χ will be positive. In a collinear

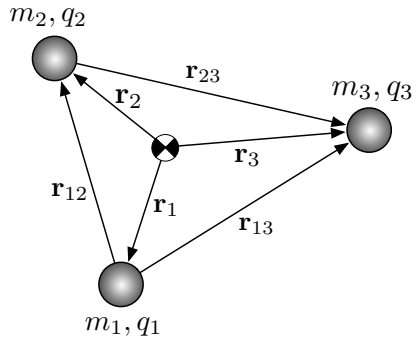

Figure 1. Three-craft Coulomb formation.

invariant shape formation, the craft will orbit about the formation center of mass on Keplerian trajectories with a time-varying angular velocity $\omega(t)$.[11] The trajectories may be circular, elliptic, parabolic, or hyperbolic and will evolve such that the craft are collinear for all time.

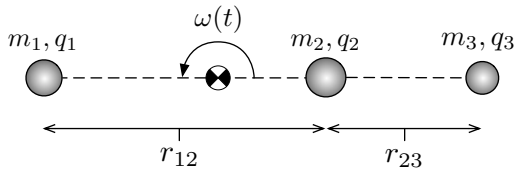

Figure 2. Collinear invariant shape Coulomb formation

In order to maintain this collinear invariant shape, the craft must be charged appropriately depending on the formation geometry and cluster angular momentum. Given a set of charges, the appropriate value of χ can be determined by satisfying the quintic equation[11]

$$\begin{aligned} 0 = &-w_2w_3\left(m_2+m_3\right) - w_2w_3\left(2m_2+3m_3\right)\chi \\ &+ \left[w_1m_1\left(w_2-w_3\right) - w_2w_3\left(m_2+3m_3\right)\right]\chi^2 \\ &+ \left[w_1w_2(3m_1+m_2) + w_3m_3(w_1-w_2)\right]\chi^3 \\ &+ w_1w_2(3m_1+2m_2)\chi^4 + w_1w_2(m_1+m_2)\chi^5, \end{aligned} \quad (2)$$

where $w_i = q_i/m_i$. Consideration of this quintic equation reveals there are six parameters which may be varied to affect the possible solutions for χ: three craft masses and three craft charges. This creates a high-dimensional search space which makes it difficult to analytically identify regions of multiple invariant shape solutions where a single set of craft charges yields multiple roots of this quintic equation. If the assumption is made that all craft are of equal mass, the quinitic equation is reduced to

$$0 = -2 - 5\chi + (\delta - \sigma - 4)\chi^2 + (4\delta + \sigma - 1)\chi^3 + 5\delta\chi^4 + 2\delta\chi^5, \quad (3)$$

where the charge ratios δ and σ are defined as

$$\delta = \frac{q_1}{q_3},\ \sigma = \frac{q_1}{q_2}. \quad (4)$$

The six-dimensional search space has thus been reduced to two; only δ and σ now affect the roots of the quintic invariant shape condition in Eq. (2) or Eq. (3). It is apparent that the coefficients in Eq. 3 are dependent only on the craft charges. Depending on the values of these charges, it may be possible to find multiple positive roots of the quintic equation. This observation was first made by Hussein and Schaub in Reference 11, though the existence of such multiple shape solutions was not determined. In their analysis, it is concluded that with the right values of σ and δ, up to three invariant shape solutions may be possible for a given set of charges. However, these are only necessary, and not sufficient conditions for multi-shape solutions. The current study resolves this issue by examining the full $\delta - \sigma$ solution space in detail.

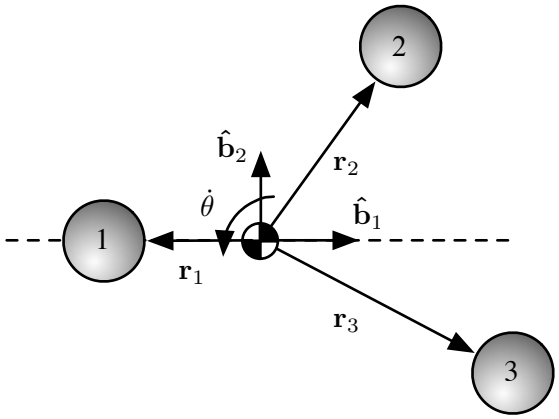

Figure 3. The rotating $\mathcal{B}$ frame.

3-Body Dynamics

To determine the stability of the equilibria of the collinear invariant shape Coulomb formation, the system dynamics are derived in a rotating coordinate frame, $\mathcal{B}$, defined by the orthogonal unit vectors

$$\mathcal{B} : \left\{ \hat{\mathbf{b}}_\mathbf{1}, \hat{\mathbf{b}}_\mathbf{2}, \hat{\mathbf{b}}_\mathbf{3} \right\}.$$

The $\mathcal{B}$ frame is aligned such that craft 1 is confined to the $\hat{b}_1$ axis for all time, while craft 2 and 3 are free to move about in the $\hat{\mathbf{b}}_\mathbf{1}$ - $\hat{\mathbf{b}}_\mathbf{2}$ plane. The origin of the $\mathcal{B}$ frame is aligned with the center of mass of the formation, and the frame rotates about this point as craft 1 moves around the center of mass. This configuration is depicted in Figure 3. The angular velocity of the $\mathcal{B}$ frame relative to the inertial frame, $\mathcal{N}$, is expressed as

$$\boldsymbol{\omega}_{\boldsymbol{\mathcal{B}}/\boldsymbol{\mathcal{N}}} = \dot{\theta}\hat{\mathbf{b}}_\mathbf{3}.$$

The kinematic equations for craft 1 in $\mathcal{B}$ frame components are

$$\mathbf{r_1} = x_1\hat{\mathbf{b}}_\mathbf{1} \tag{5}$$

$$\dot{\mathbf{r}}_1 = \dot{x_1}\hat{\mathbf{b}}_\mathbf{1} + \dot{\theta}x_1\hat{\mathbf{b}}_\mathbf{2} \tag{6}$$

$$\ddot{\mathbf{r}}_1 = (\ddot{x}_1 - x_1\dot{\theta}^2)\hat{\mathbf{b}}_\mathbf{1} + (x_1\ddot{\theta} + 2\dot{\theta}\dot{x_1})\hat{\mathbf{b}}_\mathbf{2}. \tag{7}$$

The kinematic equations for craft two and three in $\mathcal{B}$ frame components are

$$\begin{aligned}
\mathbf{r_i} &= x_i\hat{\mathbf{b}}_\mathbf{1} + y_i\hat{\mathbf{b}}_\mathbf{2} && (8)\\
\dot{\mathbf{r}}_i &= (\dot{x}_i - y_i\dot{\theta})\hat{\mathbf{b}}_\mathbf{1} + (\dot{y}_i + x_i\dot{\theta})\hat{\mathbf{b}}_\mathbf{2} && (9)\\
\ddot{\mathbf{r}}_i &= (\ddot{x}_i - x_i\dot{\theta}^2 - y_i\ddot{\theta} - 2\dot{y}_i\dot{\theta})\hat{\mathbf{b}}_\mathbf{1} + (\ddot{y}_i - y_i\dot{\theta}^2 + x_i\ddot{\theta} + 2\dot{\theta}\dot{x}_i)\hat{\mathbf{b}}_\mathbf{2}. && (10)
\end{aligned}$$

To determine the equations of motion for the craft in the formation, an expression for the electrostatic force between the craft is needed. Here, the craft are modeled as point charges in the absence of any plasma shielding effects. In Coulomb formations work these plasma effects are often considered, as they may considerably impact inter-craft electrostatic force magnitudes. See, for example, References 6, 13, and 19. In the current work, however, we neglect the partial electrostatic force shielding due to the Debye length[20] because it has a small impact on the charged relative motion considered, and the more complex expression with exponential functions prevents obtaining analytic solutions with insight into the charge-to-shape relationship. If finite Debye lengths (which model the plasma shielding effect) are included the polynomial form of Equation (3) is lost, as each of the terms will contain exponential functions. In the original work by Hussein and Schaub,[11] it is this polynomial form which allows for the application of Descartes' Rule of Signs to determine where multiple invariant shape solutions may exist. This analysis is lost if finite Debye lengths are present. Furthermore, an infinite Debye length assumption serves as a reasonable approximation if the actual Debye length is much larger than the craft separation distances. In this paper, separation distances on the order of tens of meters are considered, which does coincide with Debye lengths found in deep space. However, craft potentials on the order of tens of kilovolts are considered. At such high potentials, the effective Debye length of the local plasma environment is several times higher. This phenomen is discussed in more detail in Reference 21, where electrostatic forces are considered as a method to deflect near-earth asteroids. In the absence of plasma shielding effects, the electrostatic forces experienced on craft i in the formation are expressed as[22]

$$\mathbf{F_i} = \sum_{j=1, j\neq i}^{3} k_c \frac{q_i q_j}{r_{12}^2}\hat{\mathbf{e}}_\mathbf{ji}, \qquad (11)$$

where $k_c = 8.99 \times 10^9$ Nm/C^2 is the Coulomb constant, q_i is the charge on craft i, and $\hat{\mathbf{e}}_\mathbf{ji}$ is the unit vector from craft j to craft i. Applying the Coulomb forces to craft 1, we obtain

$$\begin{aligned}
\ddot{x}_1 &= \frac{k_c q_1}{m_1}\left(q_2\frac{x_1 - x_2}{r_{12}^3} + q_3\frac{x_1 - x_3}{r_{13}^3}\right) + x_1\dot{\theta}^2 && (12)\\
\ddot{\theta} &= -\frac{k_c q_1}{m_1 x_1}\left(q_2\frac{y_2}{r_{12}^3} + q_3\frac{y_3}{r_{13}^3}\right) - \frac{2\dot{\theta}\dot{x}_1}{x_1}. && (13)
\end{aligned}$$

Similarly, the equations of motion for craft 2 and 3 are

$$\begin{aligned}
\ddot{x}_2 &= \frac{k_c q_2}{m_2}\left(q_1\frac{x_2 - x_1}{r_{12}^3} + q_3\frac{x_2 - x_3}{r_{23}^3}\right) + x_2\dot{\theta}^2 + y_2\ddot{\theta} + 2\dot{y}_2\dot{\theta} && (14)\\
\ddot{y}_2 &= \frac{k_c q_2}{m_2}\left(q_1\frac{y_2}{r_{12}^3} + q_3\frac{y_2 - y_3}{r_{23}^3}\right) + y_2\dot{\theta}^2 - x_2\ddot{\theta} - 2\dot{x}_2\dot{\theta} && (15)\\
\ddot{x}_3 &= \frac{k_c q_3}{m_3}\left(q_1\frac{x_3 - x_1}{r_{13}^3} + q_2\frac{x_3 - x_2}{r_{23}^3}\right) + x_3\dot{\theta}^2 + y_3\ddot{\theta} + 2\dot{y}_3\dot{\theta} && (16)\\
\ddot{y}_3 &= \frac{k_c q_3}{m_3}\left(q_1\frac{y_3}{r_{13}^3} + q_2\frac{y_3 - y_2}{r_{23}^3}\right) + y_3\dot{\theta}^2 - x_3\ddot{\theta} - 2\dot{x}_3\dot{\theta}. && (17)
\end{aligned}$$

Contained in Eqs. 12- 17, then, are the dynamics of the Coulomb formation expressed in the $\mathcal{B}$ frame. Note that these equations imply an 11-dimensional state space, described by the state variables

$$\mathbf{X} = \Big[x_1,\ \dot{x}_1,\ x_2,\ \dot{x}_2,\ y_2,\ \dot{y}_2,\ x_3,\ \dot{x}_3,\ y_3,\ \dot{y}_3,\ \dot{\theta}\Big]^T.$$

The advantage of using the $\mathcal{B}$ frame is that a particular class of invariant shape solutions correspond to a single point in state space. If we consider only the case where the craft orbit about the formation center of mass on circular trajectories, the invariant shape satisfies a dynamic equilibrium such that $\dot{\mathbf{X}} = \mathbf{0}$. In order for this to be true, $\dot{x}_1 = \dot{x}_2 = \dot{x}_3 = \dot{y}_2 = \dot{y}_3 = 0$. Furthermore, all craft must lie on the $\hat{\mathbf{b}}_\mathbf{1}$ axis so that $y_2 = y_3 = 0$. To maintain the equilibrium, the craft must be positioned at finite x_i values such that the centripetal forces acting along the $\hat{\mathbf{b}}_\mathbf{1}$ axis precisely balance with the Coulomb forces acting on the craft. When this happens, $\dot{\theta}$ will be constant and the craft will maintain a circular invariant shape. At this dynamic equilibrium the state variables all take on constant values, corresponding to a single point in state space. In this manner, we have expressed the dynamics in such a way that we can use linearization to analyze the stability of a circular invariant shape solution. In limiting the analysis to circular invariant shape solutions, however, no insight is gained into the stability of the more general classes of invariant shape solutions (elliptic, parabolic, and hyperbolic trajectories).

System Constraints

As noted above, Eqs. (12)-(17) imply an 11-dimensional state space. There are a few important constraints, however, which must be considered in the analysis of this three-body system. First, consider the fact that the Coulomb forces are internal to the system. That is, the force from craft i on craft j is exactly equal and opposite of the force from craft j on craft i. If these electrostatic forces are the only forces acting on or within the system, the center of mass is inertial due to the fact that

$$M\ddot{\mathbf{R}}_c = \mathbf{F}_{ext} = 0.$$

As a result, we can always establish initial conditions which will maintain the center of mass at the origin of $\mathcal{B}$ for all time. Adopting this convention provides four constraint equations for the system,

$$\mathbf{0} = m_1\mathbf{r}_1 + m_2\mathbf{r}_2 + m_3\mathbf{r}_3 \tag{18}$$

$$\mathbf{0} = m_1\dot{\mathbf{r}}_1 + m_2\dot{\mathbf{r}}_2 + m_3\dot{\mathbf{r}}_3. \tag{19}$$

This means that at any point in time, if we know the positions and velocities of craft 1 and 2, we can compute the position and velocity of craft 3. This is significant because it allows for a reduction in state space to exclude $x_3, \dot{x}_3, y_3$ and $\dot{y}_3$.

We can reduce the state space even further using the total angular momentum. Recalling that when only Coulomb forces are acting within a formation no external forces or torques are present, we can conclude that the formation angular momentum is constant because

$$\dot{\mathbf{H}} = \mathbf{L} = \mathbf{0}.$$

Note that due to all craft motion being contained in the $\hat{\mathbf{b}}_\mathbf{1} - \hat{\mathbf{b}}_\mathbf{2}$ plane, the angular momentum will always be aligned with the $\hat{\mathbf{b}}_\mathbf{3}$ axis. If we denote the initial angular momentum as $\mathbf{H}_0$, it naturally

follows that at any time, t,

$$\mathbf{H}_0 = \sum_{i=1}^{3} \mathbf{r}_i(t) \times m_i \dot{\mathbf{r}}_i(t). \tag{20}$$

By expressing $\mathbf{r}_i$ and $\dot{\mathbf{r}}_i$ in $\mathcal{B}$ frame components, we can explicitly solve for the angular rate $\dot{\theta}$ at any point in time knowing the initial angular momentum. Contained in Eqs. (18)-(20), then, are five constraints which can be used to reduce the state space from eleven dimensions to six. The reduced state space can thus be described by the state variables

$$\mathbf{X}^* = [x_1,\ \dot{x}_1,\ x_2,\ \dot{x}_2,\ y_2,\ \dot{y}_2]\,.$$

The resulting equations of motion are

$$\ddot{x}_1 = \frac{k_c q_1}{m_1}\left(q_2 \frac{x_1 - x_2}{r_{12}^3} + q_3 \frac{2x_1 + x_2}{r_{13}^3}\right) + x_1\dot{\theta}^2 \tag{21}$$

$$\ddot{x}_2 = \frac{k_c q_2}{m_2}\left(q_1 \frac{x_2 - x_1}{r_{12}^3} + q_3 \frac{2x_2 + x_1}{r_{23}^3}\right) + x_2\dot{\theta}^2 + y_2\ddot{\theta} + 2\dot{y}_2\dot{\theta} \tag{22}$$

$$\ddot{y}_2 = \frac{k_c q_2}{m_2}\left(q_1 \frac{y_2}{r_{12}^3} + q_3 \frac{2y_2}{r_{23}^3}\right) + y_2\dot{\theta}^2 - x_2\ddot{\theta} - 2\dot{x}_2\dot{\theta}, \tag{23}$$

where

$$r_{13} = \sqrt{(2x_1 + x_2)^2 + y_2^2} \tag{24}$$

$$r_{23} = \sqrt{(x_1 + 2x_2)^2 + 4y_2^2}. \tag{25}$$

Here, the center of mass constraint has been used to eliminate the position and velocity of craft 3. The formation angular velocity can be computed at any time using

$$\dot{\theta} = \frac{m_3 H_0 + (y_2\dot{x}_2 - x_2\dot{y}_2)(m_2^2 + m_2 m_3) - m_1 m_2 (x_1\dot{y}_2 - \dot{x}_1 y_2)}{2m_1 m_2 x_1 x_2 + x_1^2(m_1^2 + m_1 m_3) + (m_2^2 + m_2 m_3)(x_2^2 + y_2^2)}. \tag{26}$$

Once initial conditions are specified, the formation angular momentum, H_0, can be computed and used throughout the simulation. Note that Eqs. (21)-(23) are solely functions of the reduced state $\mathbf{X}^*$.

Equation Linearization

To determine stability properties of a circular invariant shape solution, a linearization of Eqs. 12-15 is done about the corresponding dynamic equilibrium, $\mathbf{X}_e^*$. Using a first order Taylor series approximation, the linearized dynamics are expressed as

$$\dot{\mathbf{X}}^* = \left[\frac{\partial \dot{\mathbf{X}}^*}{\partial \mathbf{X}^*}\right]_{\mathbf{X}_e^*} \delta\mathbf{X}^*, \tag{27}$$

where δ is used to signify small perturbations about the equilibrium point. The Jacobian matrix $\left[\frac{\partial \dot{\mathbf{X}}^*}{\partial \mathbf{X}^*}\right]$ is evaluated at the equilibrium point, $\mathbf{X}_e^*$, and the eigenvalues of this matrix are computed. These eigenvalues yield insight into the stability properties of the invariant shape solution. In order for the equilibrium to be classified as stable, these eigenvalues must have negative real parts. If the linearized system has imaginary eigenvalues with no real parts we can classify the system as marginally stable in a linear sense but there is no guarantee that perturbations will not grow unstable if given enough time due to higher order terms.[23]

IDENTIFYING MULTIPLE INVARIANT SHAPE SOLUTIONS

In order to determine values of σ and δ that would yield multiple invariant shape solutions, a numerical search is performed. In Reference 11, the authors identify four cases, defined by the values of σ and δ, that impact how many potential invariant shape solutions result from a given set of charges. Using Descartes' Rule of Signs, the quintic equation is analyzed for potential sign changes, which indicates the possible numbers of positive χ roots. For illustrative purposes, the different cases are shown in Figure 4. The regions defined by these four cases are bracketed by the coefficients of χ^2 and χ^3 in Eq. (3). Following the full analysis in Reference 11, the number of possible invariant shapes for each case are found to be

Case A There will be one positive real solution, meaning one invariant shape solution.

Case B The number of real positive roots is dependent on the sign of δ. When $\delta > 0$, Eq. 3 has one positive real root and, thus, one possible invariant shape solution. When $\delta < 0$, there will be either two or no invariant shape solutions.

Case C Again, there is a dependence on the sign of δ. When $\delta > 0$, there will be one invariant shape solution satisfying Eq. 3. If $\delta < 0$, there are no possible invariant shape solutions.

Case D As before, δ is not sign definite. When $\delta > 0$, there will be either three or one invariant shape solutions satisfying the quintic equation. If $\delta < 0$, there will be either two or zero invariant shape solutions.

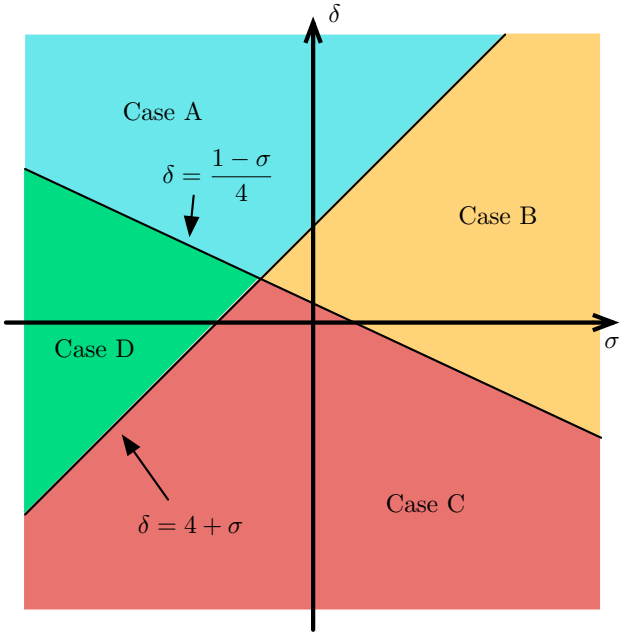

Figure 4. Different cases which affect possible numbers of positive roots of quintic equation, and thus, the number of invariant shape solutions.

These results show that there are several potential cases where multiple invariant shape solutions may be possible for a given set of charges. While their existence has been previously speculated, no actual cases were found.[11]

Search Algorithm for Multiple Solutions

For the current research, a numerical search algorithm is developed to determine the existence of constant charge multiple invariant shape solutions. In this scenario a given set of spacecraft charges can result in 2 or 3 equilibrium shapes. Using the results from the above analysis, certain regions of δ-σ space are identified and scanned using a basic grid search method. Starting at a nominal δ value, σ values are incrementally increased or decreased depending on which of the four cases is being examined, until a bifurcation into multiple invariant shape solutions is identified. Once this boundary is crossed, a simple bisection algorithm[24] is used to identify exactly where the bifurcation occurs. The search algorithm is illustrated in Figure 5. In this case, the increment on σ was set at ± 1. This allowed the algorithm to run quickly, searching a large region of space in a short period of computational time.

In both of the two cases where multiple solutions are possible (Case B and Case D), bifurcations are found by the search algorithm. These bifurcations are shown in Figure 6, where n_χ is used to denote the number of invariant shape solutions that result for a given pair of δ and σ values. Looking first at Case B, on the right side of the graph, we see that there is a large region between the boundary $\left(\delta = \frac{1-\sigma}{4}\right)$ and the point where the bifurcation occurs. No invariant shape solutions are possible in this dead space. The physical reason for this is currently under investigation. Also, note that the existence of multiple invariant shape solutions for Case B abruptly stops at $\delta = 0$. Recall that $\delta < 0$ was required for the existence of multiple solutions.

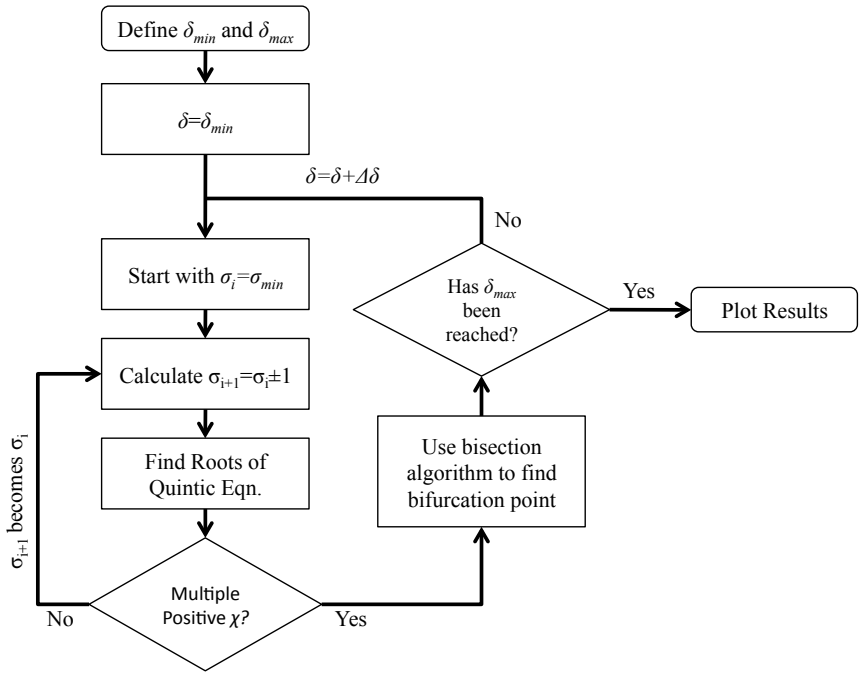

Figure 5. Search algorithm used to find multiple invariant shape solutions for a single set of charges.

Examining the results from Case D, we see that there are two separate regions of multiple invariant shape solutions, with $n_\chi = 2$ and $n_\chi = 3$. These regions are separated by the horizontal axis $\delta = 0$, which corresponds to the effects that a sign change in δ has on the possible results. Interestingly, the bifurcation is smooth across this axis even though the regions are topologically different. The reason for this is that the roots of the quintic equation enjoy partial symmetry across the δ axis. That is, for a given σ two of the roots from above the δ axis will approach the same values as those below the axis as the magnitude of δ becomes increasingly small. Consider that the limit of Eq. (3) as $\delta \to 0$ is

$$(\sigma - 1)\,\chi^3 + (-\sigma - 4)\,\chi^2 - 5\chi - 2 = 0. \tag{28}$$

On either side of the δ axis, the invariant shape solutions *must* approach the roots of Eq. (28) as $\delta \to 0$. If we apply Descartes' rule of signs, there will be two sign changes in Eq. (28) and, correspondingly, either two or zero positive roots. Because we have already identified the bifurcation into multiple invariant shape solutions, we know that there will be two positive roots. Below the δ axis, the two invariant shape solutions approach the values of these two roots as the magnitude of δ becomes increasingly small. Above the δ axis, two of the three invariant shape solutions approach these two roots, while the third approaches infinity as δ approaches zero. Like with Case B, there is a large region in Case D in between the region boundary and the bifurcation. Above the δ axis, there will be one invariant shape at any point in this region, while below the axis there will be no possible invariant shape solutions.

The results here only identify the inner boundaries of the multiple invariant shape solution regions. That is, the bifurcations identify the minimum σ magnitudes that will yield multiple solutions for a given δ value. It is not clear whether or not outer boundaries exist where multiple positive roots will no longer be possible. Numerical searches have failed to identify such a boundary out to very large magnitudes of σ, on the order of $\sigma = 10^6$, indicating that such outer boundaries are unlikely.

To illustrate physically what is meant by multiple invariant shape solutions, consider Figure 7, where circular orbits are illustrated in a non-rotating frame. Each of these invariant shape solutions corresponds to $\delta = -0.05$ and $\sigma = 7$, which leads to two roots of Eq. (3): $\chi = 3.2508,\ 4.3283$. To determine a set of charges for the craft, a charge of 10μC is assigned to craft one. The charges on craft two and three are determined using the relationships in Eq. (4). Each of these orbits corresponds to an equilibrium in our rotating $\mathcal{B}$-frame, and they both exist for the same set of charges. Note that these trajectories are generated with the same angular momentum for each χ value, so that they both belong to the same dynamical system. Examination of Figure 7 reveals slight differences between the orbits. The orbit radius for craft 1 is slightly smaller for the $\chi = 3.2508$ solution than it is for the $\chi = 4.3283$ solution. The orbit radius for craft 2, on the other hand, is slightly larger for the smaller χ value. Finally, the radius of the craft 3 orbit is nearly the same for both χ values. This particular multiple invariant shape solution is used in the next section, where a stability analysis is performed.

Resulting Orbit Types

Having identified that multiple invariant shape solutions exist for a set of constant charges, it is of interest to examine any restrictions on the resulting orbits. For example, can the orbits take on any Keplerian motion, or are they restricted solely to being on open (parabolic, hyperbolic) or closed (elliptical, circular) trajectories? To gain insight into this problem the effective gravitational parameter, μ_i, is employed. This parameter, derived in Reference 11, allows the dynamics of each

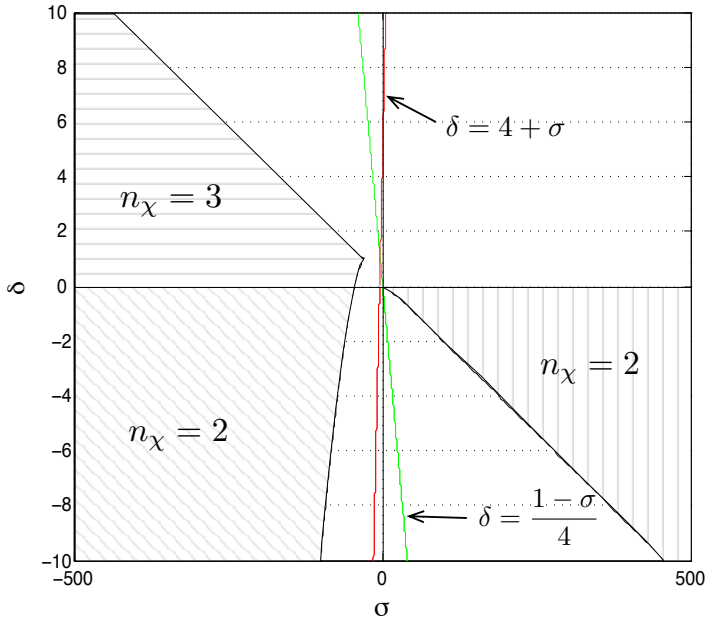

Figure 6. Bifurcations to multiple invariant shape solutions for a single set of charges found by the search algorithm.

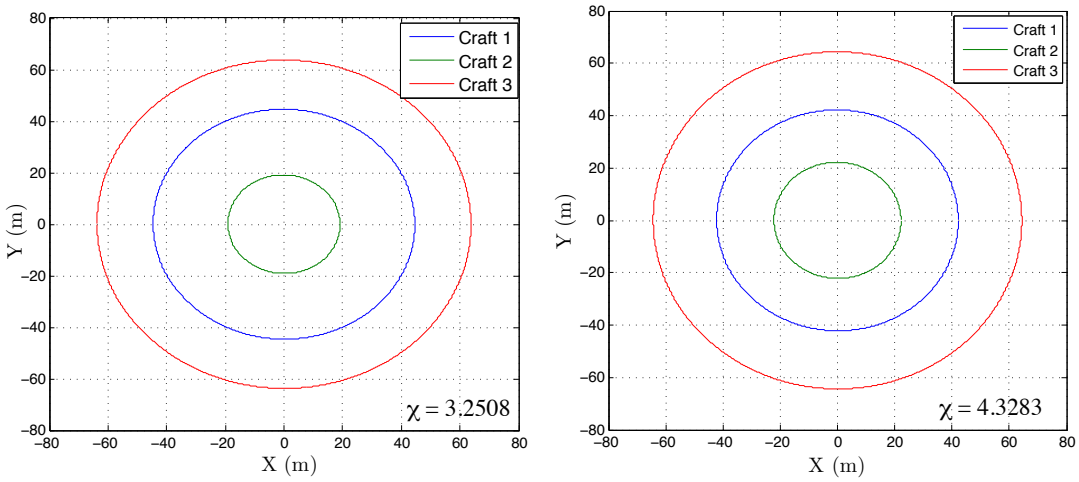

(a) χ=3.2508 (b) χ=4.3283

Figure 7. Two invariant shape solutions that exist for $\delta = -0.05$ and $\sigma = 7$.

craft in the invariant shape formation to be expressed in the form

$$\ddot{\mathbf{r}}_\mathbf{i} = -\frac{\mu_i}{r_i^3}\mathbf{r_i}. \tag{29}$$

By studying the sign of μ_i, we can obtain information on allowable orbits. If μ_i is negative then closed trajectories are not possible, as the natural dynamics of the system are repulsive. The effective gravitational parameter need only be examined for one craft, because all craft in an invariant shape

formation must be on the same trajectory type. Without loss of generality, the effective gravitational parameter of craft one will be used, which is expressed as[11]

$$\mu_1 = -\frac{k_c q_1}{\mathcal{M}_1}\left[q_2 e^{-r_{21}/\lambda_d} + \frac{q_3}{(1+\chi)^2}e^{-r_{31}/\lambda_d}\right], \tag{30}$$

where

$$\mathcal{M}_1 = \frac{m_1(m_1+m_2+m_3)^2}{m_2^2 + m_3^2(1+\chi)^2 + 2m_2m_3(1+\chi)}. \tag{31}$$

By recalling the equal mass and large Debye length assumptions, as well as the definitions of δ and σ, the effective gravitational parameter of craft one can be rewritten as

$$\mu_1 = -\frac{k_c q_1^2(2+\chi)^2}{9m(1+\chi)^2}\left[\frac{(1+\chi)^2}{\sigma} + \frac{1}{\delta}\right]. \tag{32}$$

To guarantee that closed orbits are not possible, the sign of μ_1 must be negative. In order for this to be the case, it is required that

$$\frac{(1+\chi)^2}{\sigma} + \frac{1}{\delta} > 0. \tag{33}$$

To analyze the full solution space, there are four quadrants which must be considered:

1: $\delta > 0$**,** $\sigma > 0$ It is clear that when both $\delta > 0$ and $\sigma > 0$, the inequality will hold and closed orbits will not be possible. The reason is that all craft would be charged to the same polarity, and thus experience repulsive forces. Invariant shape solutions would still be possible, but the resulting trajectories would be relegated to unbounded hyperbolic orbits.

2: $\delta < 0$**,** $\sigma < 0$ When both σ and δ are negative, the inequality will no longer be valid. Thus, closed form trajectories are possible. It should be noted that the existence of closed form trajectories does not preclude the existence of hyperbolic and parabolic trajectories. In fact, either trajectory type is possible in this situation. This case corresponds to the $n_\chi = 2$ region in quadrant III of Figure 6.

3: $\delta < 0$**,** $\sigma > 0$ No immediate insight is obtained in this case. Instead we arrive at the relation $(1+\chi)^2 > -\sigma/\delta$. Recalling Figure 6, we see that this case corresponds to the $n_\chi = 2$ region in quadrant IV. Satisfaction of the inequality is dependent on the roots of Eq. 3.

4: $\delta > 0$**,** $\sigma < 0$ In this case, we yield the inequality $(1+\chi)^2 < -\sigma/\delta$. Again, these δ and σ scenarios are inconclusive with regards to possible trajectory types. Satisfaction of the inequality depends on the roots of the quintic equation for any given σ and δ values found in the $n_\chi = 3$ region of quadrant II.

To provide insight into the resulting orbit types for cases 3 and 4, a numerical search of the solution space is performed and the resulting signs of μ_1 are computed. Using a grid search similar to that used to identify the bifurcations, the allowable orbit types are determined for the same δ and γ ranges shown in Figure 6. The results indicate that in the $n_\chi = 3$ region of quadrant II only hyperbolic trajectories are possible, while in the $n_\chi = 2$ region of quadrant IV, closed trajectories are always possible across the range of σ and δ values examined.

LINEAR STABILITY ANALYSIS

Particular Multiple Invariant Shape Case

To analyze the stability of a multiple invariant shape case, the values of $\delta = -0.05$ and $\sigma = 7$ are selected to solve the quintic necessary condition equation for an invariant shape solution. Note that these δ and σ values correspond the $n_\chi = 2$ region in quadrant IV. Thus, two positive real roots are obtained from Eq. (3): $\chi = 3.2508,\ 4.3283$. To determine the charge levels for each craft, c_1 is arbitrarily set at 10μC, and the other two charges are computed using δ and σ. In order to examine the stability of these invariant shape solutions, we first need to determine the equilibrium point in state space, which requires initial conditions. The invariant shape solution places no requirement on the actual separation distances; it only requires that the ratio remain constant for all time. Thus, we are free to choose one of the separation distances. In this case the distance between craft 1 and 2, denoted as x_{12}, is chosen. As described above, a circular invariant shape solution confines all craft to the $\hat{\mathbf{b}}_\mathbf{1}$ axis, with zero initial velocity. We only need to find the x coordinates for each craft, and the angular rotation of the $\mathcal{B}$ frame that will yield a dynamic equilibrium. Consider arbitrarily placing craft 1 at the origin (0,0) in the $\mathcal{B}$ frame. Note that for this development, we have not yet aligned the origin with the formation center of mass. With craft 1 as the rightmost craft in the formation, craft 2 and 3 would be located at $\mathbf{r}_2 = -x_{12}\hat{\mathbf{b}}_\mathbf{1}$ and $\mathbf{r}_3 = -(1+\chi)x_{12}\hat{\mathbf{b}}_\mathbf{1}$. Using the positions of the three craft, the center of mass of the formation is computed as

$$\mathbf{R}_c = -\frac{x_{12}(2+\chi)}{3}\hat{\mathbf{b}}_\mathbf{1}. \tag{34}$$

To enforce the requirement that the origin of $\mathcal{B}$ be aligned with the center of mass, we compute the compliant craft locations using

$$\begin{aligned}
\mathbf{r}_1 &= -\mathbf{R}_c \\
\mathbf{r}_2 &= -x_{12}\hat{\mathbf{b}}_\mathbf{1} - \mathbf{R}_c \\
\mathbf{r}_3 &= -(1+\chi)x_{12}\hat{\mathbf{b}}_\mathbf{1} - \mathbf{R}_c.
\end{aligned}$$

Thus, given a desired separation distance, x_{12}, we can immediately determine the equilibrium location of the craft in the $\mathcal{B}$ frame as

$$\mathbf{r}_1 = \frac{(2+\chi)x_{12}}{3}\hat{\mathbf{b}}_\mathbf{1} \tag{35}$$

$$\mathbf{r}_2 = \frac{(\chi-1)x_{12}}{3}\hat{\mathbf{b}}_\mathbf{1} \tag{36}$$

$$\mathbf{r}_3 = -\frac{(1+2\chi)x_{12}}{3}\hat{\mathbf{b}}_\mathbf{1}. \tag{37}$$

To determine the angular rate, $\dot{\theta}$, the effective gravitational parameter is used. The angular rate of a circular invariant shape formation is determined by

$$\dot{\theta} = \sqrt{\frac{\mu_i}{r_i^3}}. \tag{38}$$

Any of the craft in the formation may be used; they will all yield the same result if the craft form an invariant shape solution. Recall that while $\dot{\theta}$ does not appear explicitly in the reduced set of state variables, it is required in order to determine the initial angular momentum of the system, which

will be constant for all time. This introduces an important requirement when establishing initial conditions for the invariant shape solutions. For a proper comparison between the two invariant shape solutions, it is mandatory that both invariant shape equilibria be configured such that they have the same angular momenta. If they do not, they are different dynamical systems occupying an entirely different state space. To ensure this constraint is met, the initial conditions are set for one invariant shape formation. The angular momentum resulting from this configuration is used to determine the initial conditions for the other invariant shape solution. For a circular invariant shape solution, the angular momentum of the formation is

$$\mathbf{H} = m\dot{\theta}\left(r_1^2 + r_2^2 + r_3^2\right)\hat{\mathbf{b}}_\mathbf{3}. \tag{39}$$

In order to determine the necessary initial conditions, Newton-Raphson iteration is used on Eq. (39) to find the appropriate value for x_{12} that will yield the required momentum.

Using the above procedure, the equilibrium conditions were determined for the two invariant shape solutions under consideration. The results are summarized in Table 1. Only the six state variables and the angular momenta are presented, to correspond with the reduced state space. The position and velocity of craft 3 can be computed using the center of mass constraint. Likewise, $\dot{\theta}$ can be computed using the angular momentum from Eq. (26). Having determined the state-space equilibrium point, we can proceed to a stability analysis using the linearized equations of motion.

$\boldsymbol{\chi}$	$\mathbf{x_1}$ (m)	$\dot{\mathbf{x}}_\mathbf{1}$ (m/s)	$\mathbf{x_2}$ (m)	$\dot{\mathbf{x}}_\mathbf{2}$ (m/s)	$\mathbf{y_2}$ (m)	$\dot{\mathbf{y}}_\mathbf{2}$ (m/s)	$\mathbf{H_0}$ (kg m^2/s)
3.2508	44.616	0	19.125	0	0	0	350.972
4.3283	42.188	0	22.188	0	0	0	350.972

Table 1. Equilibrium conditions for circular invariant shapes in $\mathcal{B}$-frame components

For the numerical simulation, two different sets of equations are integrated numerically using an explicit Runge-Kutta (4,5) formula. For the rotating frame stability analysis Eqs. (21)-(23) are used, where they are linearized about the equilibrium state outlined in Table 1 to determine the eigenvalues of the equilibrium. Once the eigenvalues are determined, a perturbation of $\Delta x_1 = \Delta x_2 = -0.1$ m and $\Delta y_2 = 0.1$ m is applied and the full nonlinear equations are integrated to verify the predicted behavior. These results are used to determine the distance of each craft from its respective equilibrium point as time evolves. To determine the system response in a non-rotating frame, full inertial equations of motion are also integrated. These equations are of the form

$$m_i\ddot{\mathbf{r}}_i = \mathbf{F}_i, \tag{40}$$

where $\mathbf{F}_i$ is defined in Eq. (11). In these inertial equations, no state reduction is performed. Aside from providing craft trajectories in an inertial frame, the results also serve to verify what is obtained in the rotating-frame dynamics integration.

Considering first the case where $\chi = 3.2508$, the Jacobian matrix in Eq. (27) is computed using the equilibrium state outlined in Table 1. The resulting six eigenvalues of this matrix, presented in Table 2 , consist of three complex conjugate pairs with 0 real parts: $\pm 7.687i \times 10^{-4}, \pm 5.467i \times$

$10^{-4}, \pm 2.966i \times 10^{-4}$. In this sense, the equilibrium is expected to exhibit marginally stable behavior, implying that small perturbations will cause the craft to oscillate about the equilibrium configuration. Indeed, this behavior is observed when the nonlinear system is perturbed slightly from the equilibrium, as seen in Figure 8. As the perturbation evolves with time, the system exhibits a bounded oscillation for ten orbital periods. The symmetry observed in Figure 8(a) is a result of the center of mass constraint. Because craft 1 is confined to the $\hat{\mathbf{b}}_\mathbf{1}$ axis, craft 2 and 3 must always have y values with opposite signs and equal magnitudes. The perturbed trajectory in a non-rotating frame, determined from integration of Eq. (40), is shown in Figure 10(a). The craft largely maintain the invariant shape orbits seen in Figure 7(a), with slight oscillations.

It must be noted that the results of this linearization do not necessarily yield a full picture of the long term stability of the invariant shape. While it appears to be marginally stable for several orbital periods, it is entirely possible that higher order terms in the dynamics, as well as unmodeled perturbation effects, could cause the perturbation to grow slowly with time, ultimately resulting in instability and large scale divergence from the invariant shape equilibrium. This is a concern for any nonlinear system which has been linearized to yield purely imaginary eigenvalues.[23] The marginally stable behavior exhibited here is still a significant result, however. It is the first time a configuration of 3-craft in a Coulomb formation has been found to be marginally stable about an equilibrium.[13]

χ	**Eigenvalues**
3.2508	$\pm$ 7.687i$\times 10^{-4}$, $\pm$ 5.467i$\times 10^{-4}$, $\pm$ 2.966i$\times 10^{-4}$
4.3283	$\pm$ 9.747i$\times 10^{-4}$, $\pm$ 5.470i$\times 10^{-4}$, $\pm$ 0.3284

Table 2. Eigenvalues of Jacobian matrices for the invariant shape solutions

Considering the second invariant shape solution where $\chi = 4.3283$, the Jacobian matrix is recalculated with the parameter values in Table 1. The six eigenvalues of this matrix, shown in Table 2, consist of two complex conjugate pairs with zero real parts, and two real numbers, one positive and one negative: $\pm 9.747i \times 10^{-4}, \pm 5.470i \times 10^{-4}, \pm 0.3284$. The appearance of the real number eigenvalues means that this invariant shape solution is an unstable saddle point.[23] Small perturbations will deviate from the equilibrium and continue to grow due to this instability. This is observed using numerical simulation when the system is slightly perturbed, as seen in Figure 9. In less than one and a half orbital periods, the formation separates. Craft 2 escapes from the system, while craft 1 and 3 remain coupled, orbiting about each other. This behavior is observed in Figure 10(b), which shows the trajectories in a non rotating frame (again, determined from integration of Eq. (40)). Note how craft 2 escapes to the left, while craft 1 and 3 escape together to the right. The instability quickly disrupts the formation, and the craft diverge from the origin.

Stability Results for Other Invariant Shape Solutions

In this paper, we have examined in detail a single multiple invariant shape solution case. To provide insight into the stability properties for the different families, a numerical search is used on the δ and σ ranges shown in Figure 6 (that permit closed orbits) to identify the stability properties of the different regions. In each case of two invariant shape solutions for a single set of δ and σ, one shape is found to be unstable while the other is marginally stable. When searching regions where only one invariant shape is possible for particular σ and δ values, the shape is found to always be

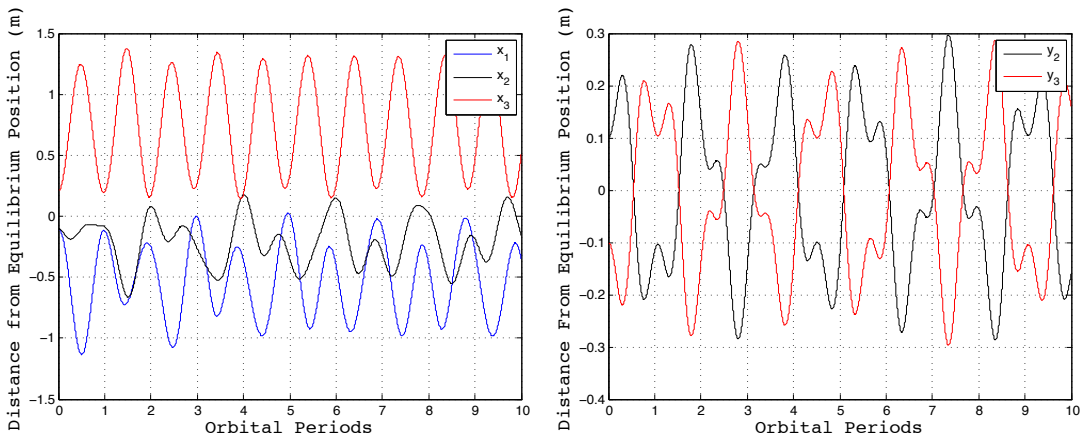

(a) x-Coordinates (b) y-Coordinates

Figure 8. Offset from equilibrium for a) x and b) y coordinates after a small perturbation for the $\chi = 3.2508$ circular invariant shape.

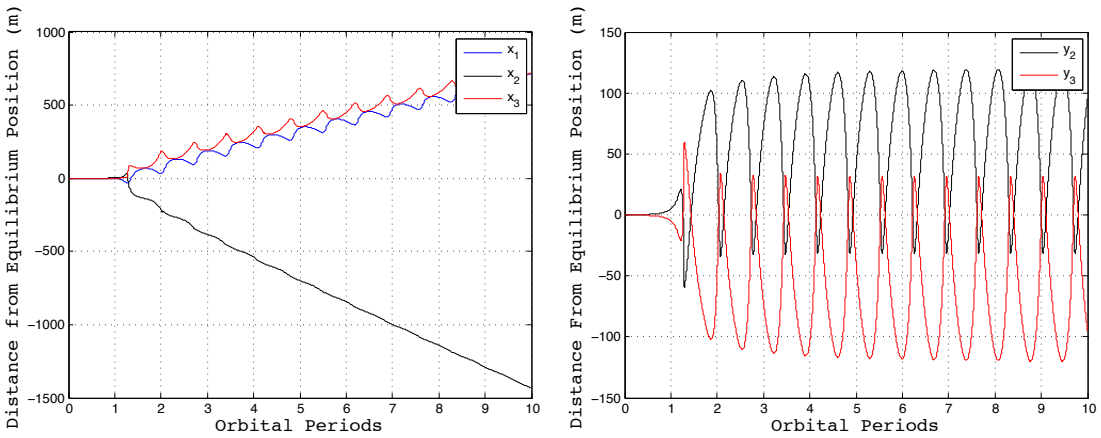

(a) x-Coordinates (b) y-Coordinates

Figure 9. Offset from equilibrium for a) x and b) y coordinates after a small perturbation for the $\chi = 4.3283$ circular invariant shape.

unstable. These results are preliminary and still under investigation.

CONCLUSION

Using a numerical search routine, families of invariant shape solutions are identified where a single set of craft charges permits multiple invariant shape solutions. Depending on the set of craft charges, anywhere from zero to three collinear invariant shape solutions are possible. This is a significant result, as it confirms speculation from earlier work[11] and provides the first examples of multiple invariant shape solutions. Furthermore, linear stability analysis has provided the first examples of marginally stable behavior for a three-craft Coulomb formation. This marginal stability appears to exist only in cases where multiple invariant shapes occur for a particular set of craft charges. When a marginally stable shape is found, it has a corresponding unstable shape for the same charge configuration. We hypothesize that in order for marginal stability to exist, the set of

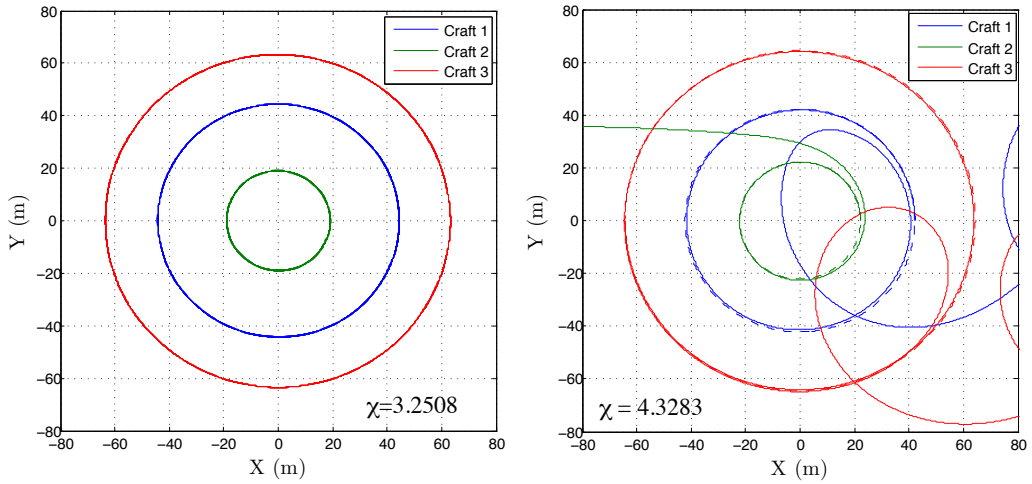

(a) $\chi = 3.2508$ (b) $\chi = 4.3283$

Figure 10. Perturbed trajectories in non-rotating frame for a) $\chi = 3.2508$ **and b)** $\chi = 4.3283$ **cases. Dashed lines represent unperturbed invariant shape orbits.**

craft charges must yield multiple invariant shapes. Resolution of this hypothesis is left for future work.

REFERENCES

[1] P. R. Lawson and J. A. Dooley, "Technology Plan for the Terrestrial Planet Finder Interferometer," Tech. Rep. JPL Publication 05-5, NASA Jet Propulsion Lab, June 2005.

[2] P. R. Lawson, O. Lay, K. J. Johnston, and C. A. Beichman, "Terrestrial Planet Finder Interferometer Science Working Group," Tech. Rep. JPL Publication 07-1, NASA Jet Propulsion Lab, March 2007.

[3] L. B. King, G. G. Parker, S. Deshmukh, and J.-H. Chong, "Spacecraft Formation-flying using Inter-vehicle Coulomb Forces," tech. rep., NASA/NIAC, available online at http://www.niac.usra.edu under "Funded Studies.", January 2002.

[4] L. B. King, G. G. Parker, S. Deshmukh, and J.-H. Chong, "Study of Interspacecraft Coulomb Forces and Implications for Formation Flying," *AIAA Journal of Propulsion and Power*, Vol. 19, No. 3, 2003, pp. 497–505.

[5] L. Pettazzi, D. Izzo, and S. Theil, "Swarm navigation and reconfiguration using electrostatic forces," *7th International Conference on Dynamics and Control of Systems and Structures in Space*, The Old Royal Naval College, Greenwich, London, England, 16-20 July 2006.

[6] H. Schaub, G. G. Parker, and L. B. King, "Challenges and Prospects of Coulomb Spacecraft Formation Control," *Journal of the Astronautical Sciences*, Vol. 52, No. 1-2, 2004, pp. 169–193.

[7] E. G. Mullen, M. S. Gussenhoven, and D. A. Hardy, "SCATHA Survey of High-Voltage Spacecraft Charging in Sunlight," *Journal of the Geophysical Sciences*, Vol. 91, 1986, pp. 1074–1090.

[8] H. B. Garrett, D. C. Schwank, and S. E. DeFrost, "A Statistical Analysis of the Low Energy Geosynchronous Plasma Environment. -I Protons," *Planetary Space Science*, Vol. 29, 1981b, pp. 1045–1060.

[9] H. B. Garrett, D. C. Schwank, and S. E. DeFrost, "A Statistical Analysis of the Low Energy Geosynchronous Plasma Environment. -I Electrons," *Planetary Space Science*, Vol. 29, 1981a, pp. 1021–1044.

[10] K. Torkar, W. Riedler, C. P. Escoubet, M. Fehringer, R. Schmidt, G. R. J. L., H. Arends, F. Rudenauer, W. Steiger, B. T. Narheim, K. Svenes, R. Torbert, A. M., A. Fazakerley, R. Goldstein, R. C. Olsen, A. Pedersen, E. Whipple, and H. Zhao, "Active Spacecraft Potential Control for Cluster – Implementation and First Results," *Annales Geophysicae*, Vol. 19, No. 10/12, 2001, pp. 1289–1302.

[11] I. I. Hussein and H. Schaub, "Invariant Shape Solutions of the Spinning Three Craft Coulomb Tether Problem," *Journal of Celestial Mechanics and Dynamical Astronomy*, Vol. 96, No. 2, 2006, pp. 137–157.

[12] E. A. Hogan and H. Schaub, "Collinear Invariant Shapes for Three-Craft Coulomb Formations," *2010 AIAA/AAS Astrodynamics Specialists Conference*, Toronto, ON, August 2–5 2010.

[13] I. I. Hussein and H. Schaub, "Stability and Control of Relative Equilibria for the Three-Spacecraft Coulomb Tether Problem," *Acta Astronautica*, Vol. 65, No. 5-6, 2009, pp. 738–754.

[14] H. Schaub and I. I. Hussein, "Stability and Reconfiguration Analysis of a Circulary Spinning 2-Craft Coulomb Tether," *IEEE Aerospace Conference*, Big Sky, MT, March 3–10 2007. Paper No. IEEEAC-1361.

[15] D. D. Dionysiou and G. G. Stamou, "Stability of Motion of the Restricted Circular and Charged Three-Body Problem," *Astrophysics and Space Science*, Vol. 152, No. 1, 1989.

[16] E. Perez-Chavela, D. G. Saari, A. Susin, and Z. Yan, "Central Configurations in the Charged Three Body Problem," *Contemporary Mathematics*, Vol. 198, 1995.

[17] F. Alfaro and E. Perez-Chavela, "Linear stability of relative equilibria in the charged three-body problem," *Journal of Differential Equations*, Vol. 245, No. 7, 2008.

[18] D. Boccaletti and G. Pucacco, *Theory of Orbits 1: Integrable Systems and Non-perturbative Methods*. New York: Springer-Verlag Berlin Heidelberg, 2004.

[19] C. R. Seubert and H. Schaub, "Tethered Coulomb Structures: Prospects and Challenges," *Journal of the Astronautical Sciences*, Vol. 57, Jan.–June 2009, pp. 347–368.

[20] D. R. Nicholson, *Introduction to Plasma Theory*. Malabar, FL: Krieger, 1992.

[21] N. Murdoch, D. Izzo, C. Bombardelli, I. Carnelli, A. Hilgers, and D. Rodgers, "Electrostatic Tractor for Near Earth Object Deflection," *59th International Astronautical Congress*, Glasgow, Scotland, 29 September-3 October 2008.

[22] J. Bittencourt, *Fundamentals of Plasma Physics*. Springer-Verlag New York, Inc, 2004.

[23] H. K. Khalil, *Nonlinear Systems*. Prentice Hall, third ed., 2002.

[24] D. V. Griffiths and I. M. Smith, *Numerical Methods for Engineers*. Taylor and Francis Group, 2006.